

HENRY

Hydraulic Engineering Repository

Ein Service der Bundesanstalt für Wasserbau

Conference Paper, Published Version

Eden, Derek; Douglas, Steven; Simpalean, Adrian; Kozlowski, Tom; Nistor, Ioan; Cornett, Andrew; Anglin, Dave; Via-Estrem, Lluís; Latham, J. P.; Xiang, Jiansheng

Quantifying Forces and Pressures on Core-Loc™ Armour Units via Instrumented Units and Image Processing

Verfügbar unter/Available at: <https://hdl.handle.net/20.500.11970/106622>

Vorgeschlagene Zitierweise/Suggested citation:

Eden, Derek; Douglas, Steven; Simpalean, Adrian; Kozlowski, Tom; Nistor, Ioan; Cornett, Andrew; Anglin, Dave; Via-Estrem, Lluís; Latham, J. P.; Xiang, Jiansheng (2019): Quantifying Forces and Pressures on Core-Loc™ Armour Units via Instrumented Units and Image Processing. In: Goseberg, Nils; Schlurmann, Torsten (Hg.): Coastal Structures 2019. Karlsruhe: Bundesanstalt für Wasserbau. S. 116-126.
https://doi.org/10.18451/978-3-939230-64-9_013.

Standardnutzungsbedingungen/Terms of Use:

Die Dokumente in HENRY stehen unter der Creative Commons Lizenz CC BY 4.0, sofern keine abweichenden Nutzungsbedingungen getroffen wurden. Damit ist sowohl die kommerzielle Nutzung als auch das Teilen, die Weiterbearbeitung und Speicherung erlaubt. Das Verwenden und das Bearbeiten stehen unter der Bedingung der Namensnennung. Im Einzelfall kann eine restriktivere Lizenz gelten; dann gelten abweichend von den obigen Nutzungsbedingungen die in der dort genannten Lizenz gewährten Nutzungsrechte.

Documents in HENRY are made available under the Creative Commons License CC BY 4.0, if no other license is applicable. Under CC BY 4.0 commercial use and sharing, remixing, transforming, and building upon the material of the work is permitted. In some cases a different, more restrictive license may apply; if applicable the terms of the restrictive license will be binding.



Quantifying Forces and Pressures on Core-Loc™ Armour Units via Instrumented Units and Image Processing

D. Eden^{1,3}, S. Douglas¹, A. Simpalean¹, T. Kozlowski¹, I. Nistor¹, A. Cornett^{1,2},
D. Anglin³, L. Via-Estrem⁴, J.P. Latham⁴, J. Xiang⁴

¹University of Ottawa, Ottawa, Canada

²National Research Council of Canada, Ottawa, Canada

³W. F. Baird & Associates Coastal Engineers Ltd., Ottawa, Canada

⁴Imperial College London, London, England

Abstract: The paper will present the results of an experimental program investigating the impact of waves on concrete armour units used for the construction of rubblemound breakwaters. The current study is part of a collaboration between researchers from the University of Ottawa (uOttawa), National Research Council of Canada – Ocean, Coastal and River Engineering Research Centre (NRC-OCRE), Imperial College London (ICL), and W.F. Baird & Associates Coastal Engineers Ltd. (Baird). A Core-Loc™ armour unit was 3D printed at the University of Ottawa MakerSpace, instrumented with six pressure sensors and mounted on a force transducer in a wave flume at NRC-OCRE. Following testing and calibration, the instrumented unit was placed on a rigid impermeable slope and exposed to a wide range of wave conditions to investigate the hydrodynamic loading due to waves and to investigate the sensitivity to various wave conditions and unit placement locations. Results from the unit testing and calibration showed that the instrumented Core-Loc™ armour unit was capable of measuring pressures up to 27,000 Pa, at a resolution of 1.2 Pa, with a total combined error of 0.53% and at sampling rates up to 320 Hz. The results of the wave experiments showed that decreasing surf similarity parameter and increasing wave steepness were correlated with increased forces and pressures on the unit. The results also showed that units located below the still water level experience the highest loads during wave impact. The methodology and results of the current study help to better understand armour unit hydrodynamics, advance rubblemound breakwater design towards a force-balance type approach and provide unique experimental datasets for the calibration and validation of numerical models.

Keywords: breakwater, rubblemound, image processing, concrete armour unit, Core-Loc™, wave-structure interaction, hydrodynamics, instrumentation, forces, pressures

1 Introduction

Rubblemound breakwaters are often the first and last lines of defense protecting shorelines, ports and other coastal infrastructure. Despite widespread use, the interaction between waves and armour layers is not well understood. Consequently, the detailed force-balance design approach typically applied in design of most civil engineering structures is not applied when designing breakwaters. The complex nature of the wave-structure interaction has rendered assessment of forces acting on individual armour units impractical, and without a force-balance design approach, coastal engineers have relied on empirical design techniques developed through extensive experimental testing at reduced scale and analysis of past case studies. The current design process lacks the quantification of unit forces, concrete stresses and hydrodynamic pressures. Additionally, secondary effects such as unit movements, unit collisions, concrete fatigue, debris impacts and other design related factors are often not considered.

Several studies have been undertaken in an effort to better understand the behaviour of armour units during wave action, and to develop more comprehensive design methods. The current study draws inspiration from similar, yet distinct, studies aimed towards quantifying the complex hydrodynamic forcing and response of armour units, such as: Burcharth (1985), Scott et al. (1988),

Sakakiyama and Kajima (1990), Van der Meer et al. (1994), Cornett (1995), Douglas et al. (2018), Hofland et al. (2018), and others.

2 Research Motivation and Novelty

The principle motivation of the current study is to develop techniques to better understand the hydrodynamic loads on armour units due to wave action, and to advance development of a force balance design approach for rubble mound breakwaters. Additionally, this study aims to provide insight and ideas for future similar works that will introduce a new type of measurement technique using instrumented “Smart-Units”.

The primary objective of the current study is to use these techniques to quantify the hydrodynamic forces and pressures exerted on armour units during wave action, and to assess the performance of instrumented “Smart-Units” in an idealized breakwater setting, prior to more complex testing. The secondary objective is to obtain force and pressure readings on a single armour unit across a wide range of wave conditions and to isolate the effect of different wave conditions and armour unit locations relative to the still water level (SWL).

The novelty of the current study lies in the development of innovative measurement techniques that enabled the acquisition of unique datasets describing the loading on a single isolated armour unit located on an impermeable slope. The techniques provide quantitative measurements of wave pressures and forces that were previously unavailable. Not only can these measurement techniques provide useful information for improving breakwater design methods, but they also provide data to support calibration and validation of numerical models capable of accurately simulating wave interactions with rubblemound breakwaters. The team at ICL has developed a novel coastal modelling tool, Latham et al. (2013), and intend to use experimental data produced from these experiments for calibration and validation purposes.

3 Experimental Methodology

3.1 Instrumented Core-Loc™ Armour Unit

3.1.1 Unit Development

At the uOttawa MakerSpace, a Core-Loc™ armour unit was 3D printed using PLA plastic such that pressure sensors (Honeywell TBF-LPNS001BGUCV) could be embedded into the surface of the armour unit. A semi-hollow core was included in the design in order to allow for self-containment of differential signal amplifiers (Texas Instruments INA155U), analog-to-digital converters (Adafruit ADS-1115), and associated circuitry. The unit also contained multiple locations for embedment of coupling nuts to allow the unit to be mounted onto a force transducer at various unit orientations. A small wire connected the unit to a Raspberry Pi 3 Model B (RPi3), a credit card sized fully functional Linux based computer. The RPi3 powered the internal circuit, acted as the data-acquisition-system (through a specially developed Python interface), and could transmit data in real time via Wi-Fi. The process of constructing the unit, outfitting it with instrumentation and data acquisition systems, and the resulting unit is depicted in Fig 1.

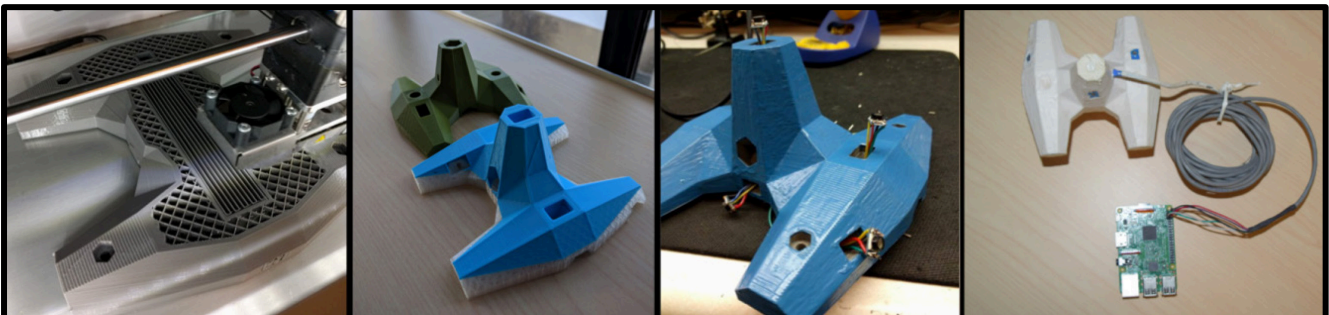


Fig. 1. Printing of unit (1), Printed unit (2), Circuit Assembly (3), Final instrumented unit (4).

The resulting unit had a height of 0.12 m and was fitted with six pressure sensors at locations chosen to best represent the full range of pressures acting on the unit's surface, while accounting for printing and wiring logistics. The locations of the embedded pressure sensors are shown in Fig. 2, while Tab. 1 lists the coordinates of each pressure sensor relative to the centroid of the unit.

Tab. 1. Instrumented Core-Loc™ Unit Pressure Sensor Locations

Location	X (mm)	Y (mm)	Z (mm)
Centroid	0.00	0.00	0.00
P1	-60.00	0.00	0.00
P2	-14.00	-28.00	-34.00
P3	-22.00	39.25	0.00
P4	12.00	52.00	26.00
P5	36.00	0.00	-16.25
P6	19.00	-39.25	22.00

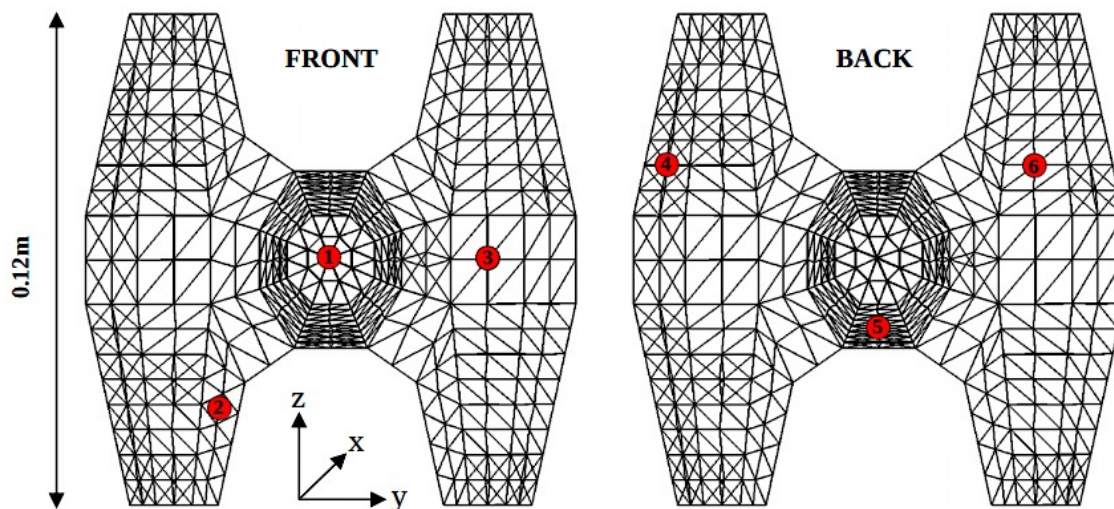


Fig. 2. Distribution of Pressure Sensors on Instrumented Core-Loc™ Unit Surface.

3.1.2 Unit Testing and Calibration

All initial testing and calibration of the instrumented unit was performed at the uOttawa Hydraulics Laboratory, in a 2.5 m tall x 0.56 m diameter vertical drop-tank. The unit was mounted on a threaded rod, which was then fixed to an adjustable frame atop the drop-tank. This configuration allowed for a range of constant and desired submergence depths.

In order to perform in an experimental breakwater setting, the unit must be able to withstand variable levels of submergence for extended periods of time. To test the unit's performance in this respect, the unit was first submerged at a constant 2 m depth for over 48 hours. During this period, the signal of each pressure sensor was carefully monitored to ensure its' reliability during long periods of submergence.

Following this initial testing, specific protocols were followed to determine the general operating characteristics, calibrate the unit output, and to quantify the accuracy of measurement. The protocols were designed to measure the sensitivity, repeatability, non-linearity, and hysteresis characteristics of the pressure sensors. In addition, the minimum threshold pressure, ambient signal noise, zero drift, output resolution, and sampling frequency of the pressure sensors were determined.

3.2 Single Unit Tests

3.2.1 Flume Setup

The objective of this portion of the current study was to evaluate the performance of the instrumented unit in an idealized breakwater setting, and to obtain and analyze measurements to isolate the effects of different wave conditions and unit placement locations on the hydrodynamic forces and pressures.

The tests were performed at the NRC-OCRE lab in Ottawa in a 60 m x 1.22 m x 1.22 m steel wave flume fitted with glass side walls. A hinged support frame with a smooth, impermeable surface was constructed that allowed for different breakwater slopes and various unit locations to be tested. The slope was kept constant at 4H:3V, and tests were conducted with the unit at three locations: at the SWL, 0.259 m above the SWL and 0.259 m below the SWL in the slope parallel direction. The breakwater slope and unit locations were chosen based on consideration of Core-Loc™ manufacturer design guidelines, CLI (2012). One unit orientation was tested, as the effect of Core-Loc™ unit orientation was previously investigated through this same collaboration (Douglas et al., 2018). As part of the idealized nature of this stage of testing, the unit was placed isolated and unprotected on the slope. This simplified setup was used to assess the performance of the instrumented unit before moving to more complex testing with full armour layers. Sketches of the flume setup and three unit locations are shown in Fig. 3 and Fig. 4.

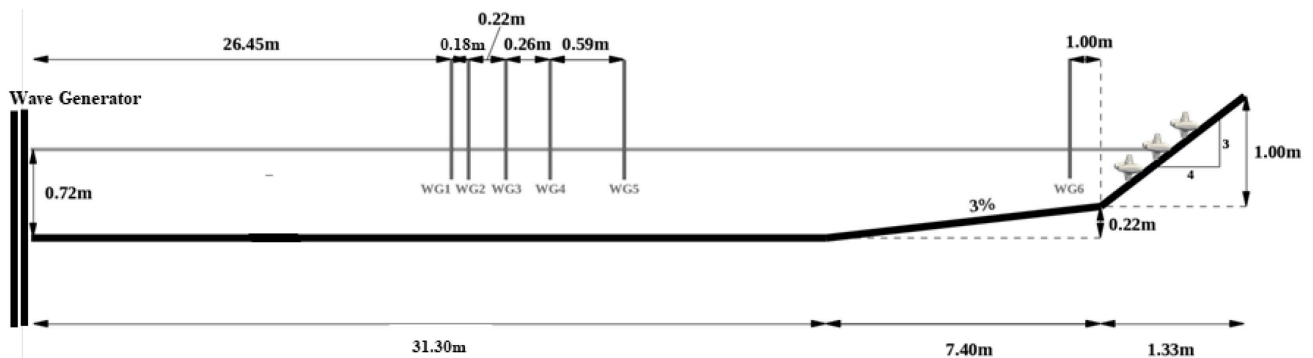


Fig. 3. Experimental Flume Setup at NRC-OCRE (not to scale).

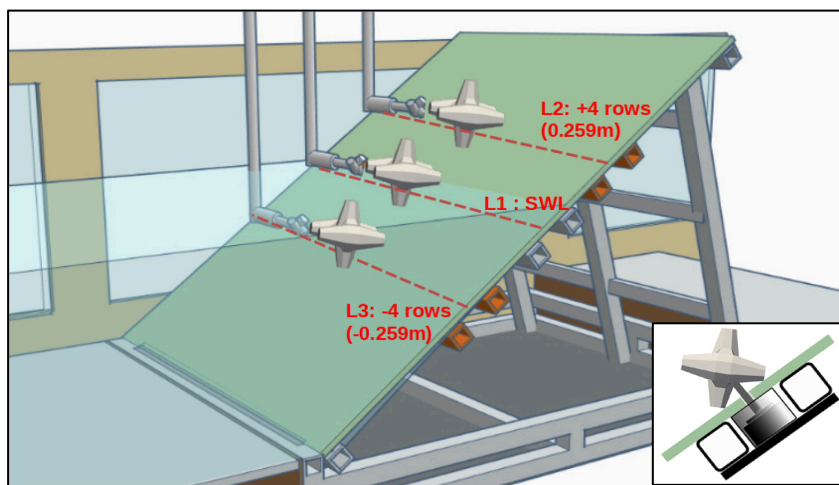


Fig. 4. Schematic of Breakwater Slope and Unit Testing Locations (L1 = SWL, L2 = upper, L3 = lower) with inset figure showing the force transducer and unit mounting system.

3.2.2 Instrumentation and Measurement

The instrumented Core-Loc™ unit provided pressure measurements at six different locations on the unit's surface. In addition, the unit was mounted on a six degree-of-freedom force transducer (model ATI Mini45 IP68) to record forces and moments acting on the unit during testing. Capacitance type wave gauges were utilized to record the time-histories of water surface elevation, from which wave heights and periods were determined. Five wave gauges were positioned in an array starting 12.25 m offshore from the breakwater toe, and one was located 1 m offshore of the breakwater toe. A Nortek Acoustic Doppler Velocimeter (ADV) was used to measure fluid velocities near the instrumented unit. The instrumentation and locations are shown in Fig. 3 and Fig. 4.

In addition to the instrumentation described above, a novel image processing technique was developed to track the water surface at the breakwater location. A Nikon D5300 DSLR camera was used to record, through the side glass wall of the flume, the water surface during each test at 1920 x

1080 pixel resolution, with a framerate of 30 Hz. The instrumented unit was painted white, a white background was positioned behind the unit, and a lighting arrangement was installed to promote a high contrast between the water surface and the white background. The water surface delineation on the breakwater slope was achieved through the implementation of a single-value threshold technique that was based on grayscale pixel intensity of images that were converted from RGB. The delineated water surface was then converted to a representative 3D mesh. This mesh was then used to perform a Boolean intersection operation on a representative mesh of the unit which enabled the estimation of the submerged portion of the unit at any given time during testing, and consequently, the time-varying buoyancy force acting on the unit. The buoyancy force was then decomposed into its X (slope parallel) and Z (slope normal) components based on the breakwater slope. The authors could therefore subtract the effect of buoyancy from the total forces acting on the unit in order to isolate the remaining hydrodynamic forces. A visualization produced using this image processing technique is shown in Fig. 5.

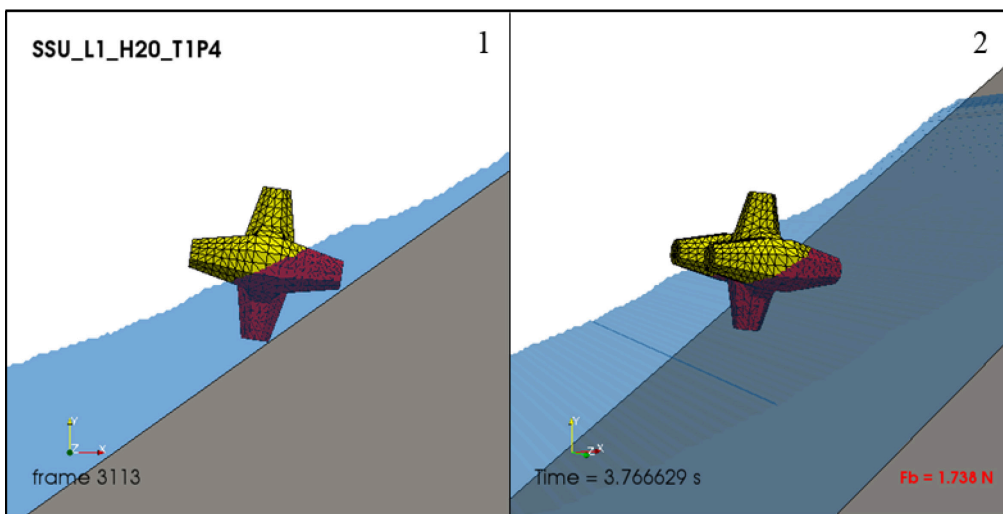


Fig. 5. 3D Rendering of Image Processing Results for Sample Test Condition - side view (1) and skewed view (2)

3.2.3 Testing Conditions

This portion of the experimental program consisted of exposing the instrumented unit to 14 regular and 4 irregular wave conditions which were performed at all three unit locations, resulting in 54 tests. Tests with regular waves were run for 210 seconds, while tests with irregular waves were run for 900 seconds. The range of regular and irregular wave conditions are summarized in Tab. 2. These conditions were chosen based on the wave-maker capabilities and the desire to investigate a large range of wave conditions that would produce a range of breaker types including plunging, collapsing and surging. The maximum wave conditions approached design conditions (assuming a geometric model scale of 1:25) as per manufacturer preliminary design guidelines, CLI (2012).

Tab. 2. Summary of Wave Conditions for Experimental Tests

Wave Type	Parameter	Notation	Range	Units
Regular	Height	H	0.12 - 0.20	m
	Period	T	1.4 - 3.8	s
	Steepness	s_0	0.007 - 0.07	-
	Surf Similarity	ξ_0	2.9 - 9.2	-
Irregular	Height	H_{m0}	0.15	m
	Period	T_p	1.4 - 2.6	s
	Steepness	$s_{m-1,0}$	0.01 - 0.06	-
	Surf Similarity	$\xi_{m-1,0}$	3.2 - 6.9	-

4 Results

4.1 Instrumented Core-Loc™ Armour Unit

Results from the initial submergence testing showed that the instrumented unit design, and associated circuitry, performed reliably and provided accurate and constant output for periods exceeding 48 hours at submergence depths of up to 2 m. This was well outside the range of intended testing durations and water depths and the unit was thus deemed acceptable for use in a flume setting.

The sensitivity of the pressure sensors was determined through a protocol to generate the sensor calibration curves, shown in Fig. 6. This protocol involved recording pressures during vertical movement of the instrumented unit at known submergence depths. As expected, the sensitivity of the various sensors was nearly identical and closely followed manufacturer's specifications. While each sensor had a slightly different zero reading, the calibration coefficients differed by less than 1%. The non-linearity of the pressure sensors was determined through comparison of the calibration coefficient to the raw calibration curves. It was found that the pressure sensors had an error of 0.009%, on average, due to this effect. The hysteresis error was determined by monitoring the sensor output during cyclical excitation and was found to be less than 0.6% for all sensors. The minimum threshold reading occurred immediately upon submergence and was assumed to be 0 Pa for all sensors. The zero reading of the pressure sensors was found to drift slightly from day to day but was easily accounted for by re-zeroing the sensors before use. Each sensor was found to have signal noise in the range of ± 20 Pa concentrated around the 4-8 Hz frequency band. This was removed using a spectral band-pass filter. This signal noise was likely due to ambient electromagnetic conditions, the proximity of multiple wires and instruments within the unit's hollow cavity, and gaps in the shielding.

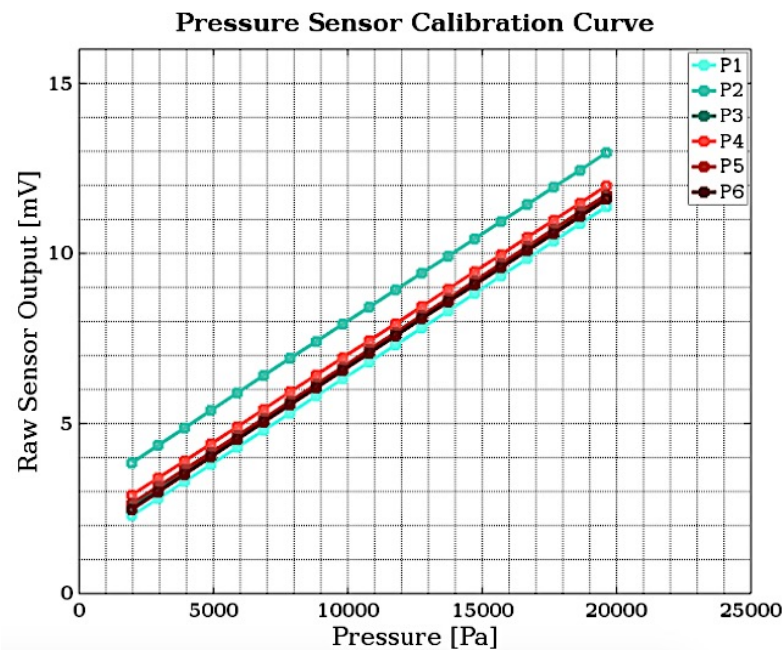


Fig. 6. Pressure Sensor Calibration Curves.

Through analysis of the results from the initial testing and calibration protocols, it was determined that each sensor was able to detect pressure fluctuations with magnitudes up to 27,000 Pa with a total combined error of 0.53% (on average). Each sensor could be sampled at frequencies ranging from 50-320 Hz, depending on the number of sensors being sampled, at a resolution of approximately 1.2 Pa (after noise removal).

4.2 Single Unit Tests

While there was a marked difference in the magnitude and shape of the recorded force and pressure time histories depending on the wave conditions, similar trends were observed in each of the tests. Five distinct events or phases of hydrodynamic loading were observed during each wave cycle. These are denoted as dashed vertical lines in Fig. 7, which presents the Z-axis (slope-normal) forces and

pressures measured by two sensors for regular waves with $H = 0.12$ m and $T = 2.0$ s on the unit installed at the L1 (SWL) location. In Fig. 7, F_z denotes the slope-normal component of the measured force, F_{Bz} denotes the estimated buoyancy force in the slope-normal direction, and F_{Hz} denotes the hydrodynamic force in the slope-normal direction (estimated by subtracting F_{Bz} from F_z). For each wave cycle, there is a period where the water level on the slope drops below the unit, the unit is not submerged, and both the pressures and forces approach zero (T1). Following this, a high velocity jet (resulting from wave breaking) impacts the front of the unit as the bulk of the run-up lags behind. This results in peak pressures on the front (down-slope side) of the unit and marks the beginning of a rapid increase in both total and buoyant forces (T2). The impulsive peak pressure was lower in magnitude and less distinct in less extreme wave conditions. The run-up then impacts and envelops the unit, which results in a secondary, lower peak pressure occurring on the front of the unit. This also leads to maximum total, hydrodynamic and buoyant forces as the unit becomes fully submerged (T3). Pressures on the back (up-slope side) of the unit began to rise at this point. Run-up would then reach its maximum level, followed by flow reversal. This stage of flow reversal results in hydrodynamic forces approaching zero, with total forces approaching the magnitude of the buoyant forces (T4). During run-down, as the water flows down the slope and past the unit, both the total and hydrodynamic forces peak in the negative direction (into the slope), while the pressures on the back (up-slope side) of the unit reach its maximum (T5). Following this, buoyancy force decreases to zero as the water surface falls below the unit. All forces and pressures would then approach zero and repeat the same loading behaviour for the next wave cycle.

As mentioned previously, a total of 54 unique datasets were collected during this stage of the experimental program. In addition, each test was repeated at least once, and the tests with largest ($H = 0.20$ m) wave conditions were repeated up to five times. In order to consolidate the large amount of data collected for various wave conditions and unit locations, a statistical analysis of peak forces and pressures during each test was performed to extract key statistics to describe each dataset. These values could then easily be plotted and compared; this approach made it more efficient to distinguish relationships between force, pressure, unit location, and wave conditions on a large scale. For regular waves, the peak forces in both positive and negative directions were extracted for each wave cycle, along with peak pressures on the front (down-slope side) and back (up-slope side) of the unit. Similar peak data was extracted for irregular wave tests using a peak-over-threshold method. Peak forces were non-dimensionalized by dividing the force by submerged unit weight (W'), assuming a unit density representative of concrete, 2400 kg/m^3 .

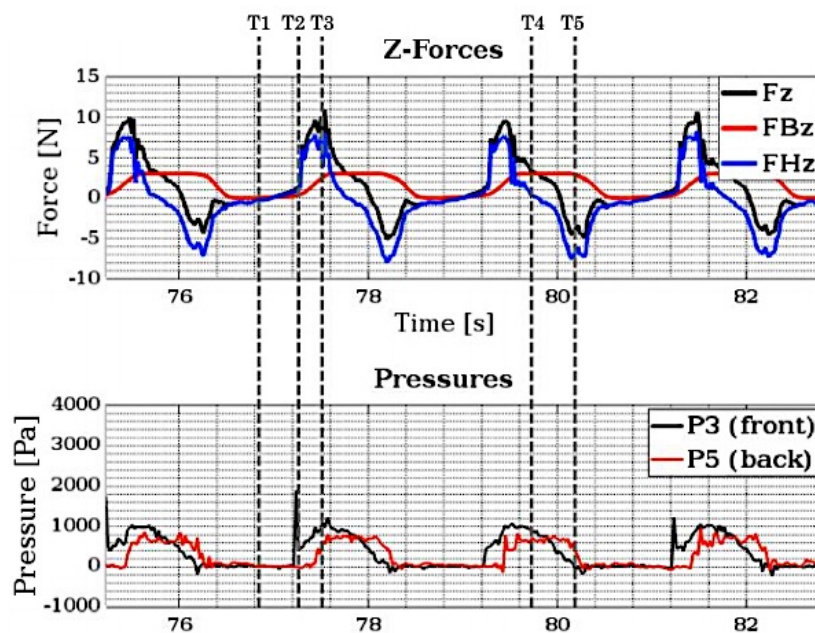


Fig. 7. Z-force (slope normal) and Pressure Time History for Location L1; Wave Height $H=0.12\text{m}$ and Period $T=2.0\text{s}$

Due to the wide range of wave conditions tested, it was possible to investigate the effect of wave steepness while keeping wave height constant. Fig. 8 shows the relationship between wave steepness and peak hydrodynamic forces in both positive X (slope parallel) and positive Z (slope normal) directions for wave conditions with heights of 0.12 m and 0.15 m. For all unit locations, it was observed that induced hydrodynamic forces in both directions increased as wave steepness increased. This effect was apparent but significantly reduced at the L2 unit location (4 rows above SWL). These findings are in agreement with conclusions reached by Van der Meer (1988) and correlate directly with results presented by Sakakiyama and Kajima (1990). Interestingly, the results indicate that peak hydrodynamic X-forces (and total X-forces, not shown) on the unit located at the L3 location (4 rows below SWL) exceed the peak forces observed for the unit placed at the L1 location (SWL) for the most extreme wave conditions (i.e. high steepness). Also, the results indicate that peak Z-forces for these locations appear to have similar magnitude. This result implies that, for certain wave conditions, the largest hydrodynamic loads with potential to destabilize a unit occur at locations below the SWL. This is in agreement with results presented by Cornett and Mansard (1994) and Hofland et al. (2018).

In order to visualize the effect of surf similarity parameter on the 54 unique datasets simultaneously, a modified surf similarity parameter was proposed and is presented in Eq. (1):

$$\xi_0 d L_0 / H^2 \quad (1)$$

where ξ_0 = surf similarity ($\xi_{m-1,0}$ for irregular waves), d = toe water depth, L_0 = deep water wavelength and H = wave height (H_{m0} for irregular waves). This modified surf similarity parameter was used to analyze waves that may have comparable surf similarity parameters but that resulted in different force and pressure magnitudes due to different wave heights and allowed for better comparison. For example, regular waves with $H = 0.12$ m and $T = 1.8$ s corresponds to $\xi_0 = 4.9$ while regular waves with $H = 0.15$ m and $T = 2.0$ s corresponds to $\xi_0 = 4.8$ which are similar, but each produce different force and pressures.

Fig. 9 shows the effect of surf similarity on the induced peak pressures recorded on the front (down-slope side) and back (up-slope side) of the unit for all test conditions with the unit placed at the L1 (SWL) location. The magnitude of peak pressures tends to increase as the surf similarity parameter magnitude decreases. Intermittent peak pressures on the front (down-slope side) of the unit during irregular wave tests exceeded the pressures observed during the regular wave tests. This behaviour was also observed on the back (up-slope side) of the armour unit, except for the irregular wave condition with $T_p = 1.4$ s. This anomaly can be attributed to the large amount of energy dissipated during the wave breaking process and less extreme run-down behaviour acting on the unit for this test.

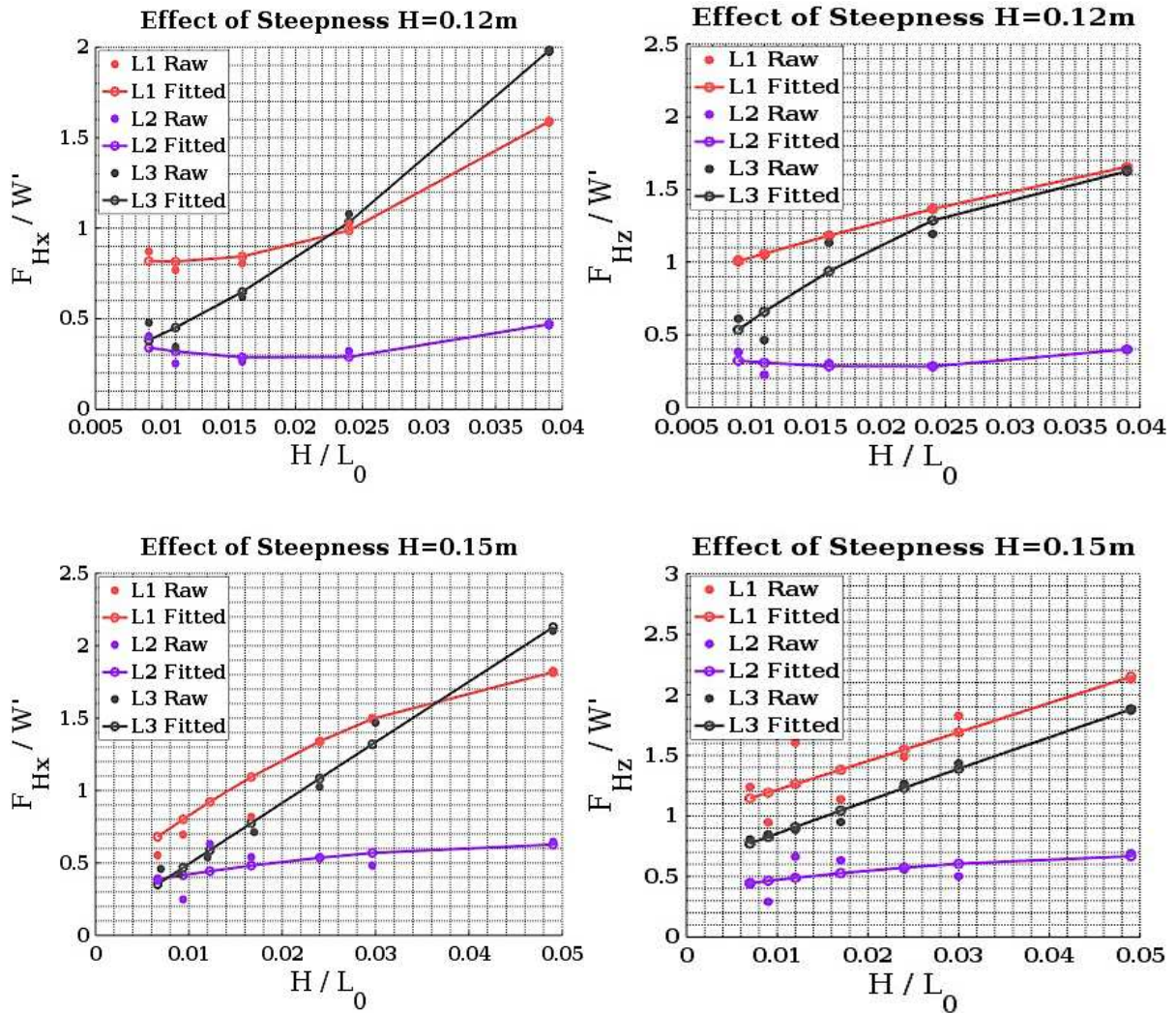
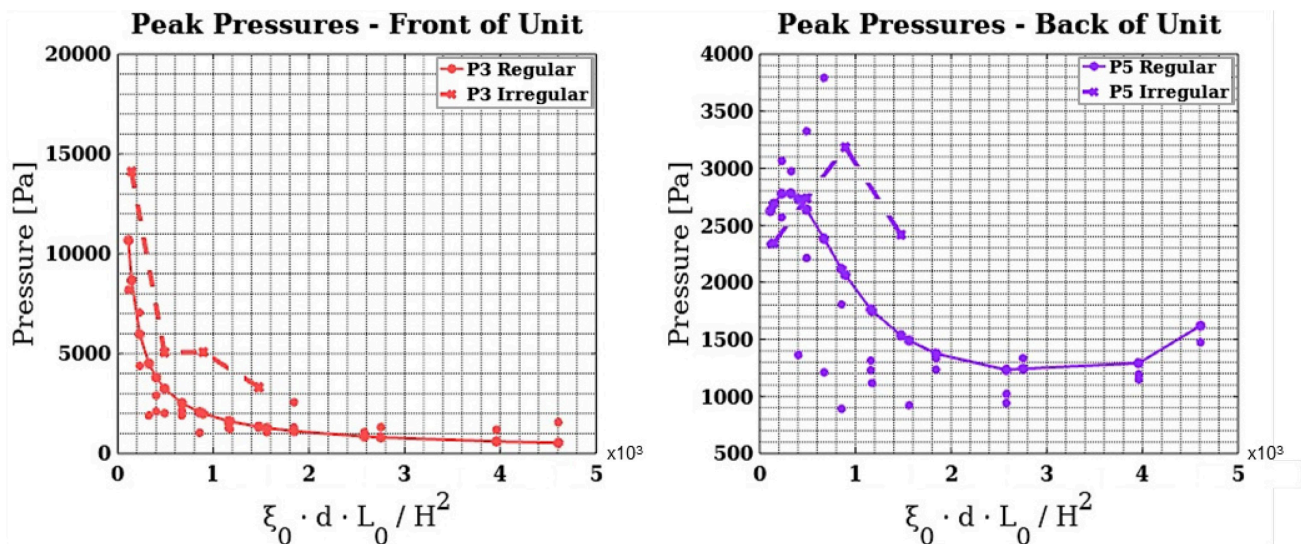


Fig. 8. Non-dimensionalized Hydrodynamic X-Forces (left) and Z-forces (right) vs. Wave Steepness for all Testing



Locations, for Regular Waves with $H = 0.12\text{ m}$ and $H = 0.15\text{ m}$.

Fig. 9. Peak Pressures on the Front (P3, left) and Back (P5, right) of Unit vs. Modified Surf Similarity Parameter for all Regular and Irregular Wave Conditions at SWL (L1) Testing Location.

5 Conclusions

The results of the current study show that the era of using instrumented “Smart-Units” for experimental testing of breakwater armour units has arrived and that this approach can provide valuable insights into the hydrodynamic interaction between waves and armour units. This technique provided reliable measurements revealing the effect of different wave conditions and unit locations on the hydrodynamic loading and pressures acting on a single isolated Core-Loc armour unit on a smooth impermeable slope. This study demonstrates that widely available, low-cost, relatively low-tech instrumentation can contribute to advancing knowledge of the loads acting on armour units under wave action, provide valuable data to support development of predictive numerical tools, and contribute to advancing design techniques towards a force-balance approach. These techniques have been expanded by the authors to investigate the impact of waves on armour units in more complex and realistic conditions in a multi-unit armour layer (Douglas et al., 2019).

In the NRC-OCRE flume tests, a newly developed image processing technique capable of accurately tracking the water surface profile above a breakwater slope was applied to provide reasonably accurate estimates of the time-varying buoyancy force.

A statistical analysis was performed on the measured force and pressure signals in order to extract key information and reduce the datasets to representative values to facilitate further analysis and comparison. The results showed that, for a constant wave height, a reduction in surf similarity parameter resulted in an increase of generated forces in both the X (slope-parallel) and Z (slope-normal) directions (both positive and negative); this included both total and hydrodynamic forces. Pressure readings in all sensors also increased as a result of decreasing surf similarity parameter.

Wave steepness appears to have a strong influence on the hydrodynamic loading. Increased wave steepness for a given wave height correlated with increased total and hydrodynamic forces and pressures. This is in agreement with the findings of Sakakiyama and Kajima (1990), Van der Meer (1988) and other similar studies and design formulations.

The data obtained in this study indicates that, under certain wave conditions, units placed below the SWL (L3) were subjected to the highest loads. This result confirms results proposed by Cornett and Mansard (1994) and Hofland et al. (2018).

6 Recommendations for future work

Additional breakwater design parameters such as toe water depth, packing density, different placement grids, structure permeability, and unit scale would provide valuable information for advancing current rubblemound breakwater design techniques. For future testing into the investigation of the effect of unit location on the slope, it is recommended that adjacent rows be chosen closer together. In addition, it is recommended to have more data points below the SWL to capture the unique behaviour in this area. In order to more accurately capture the effect of buoyancy in future testing, a 3D image processing technique could be employed, or an array of water level sensors could be placed around the unit to accurately record the 3D time-history of the water surface.

In order to maintain long-term integrity of the pressure sensors, it is recommended to ensure the sensors are slightly recessed into the unit, or somehow protected if they are flush with the surface. The coupling nuts used to mount the unit on the force transducer can be replaced with low-cost accelerometers and gyroscopes, as in Van der Meer and Heydra (1991) and Hofland et al. (2018). Smaller versions of the RPi3 exist, as well as smaller, more specialized microcontrollers. Further development in this respect can reduce unit scale, increase measurement accuracy, and increase sampling frequency. Embedding this system directly into the armour unit for future versions would allow all instrumentation to be contained in either specially crafted concrete or machined metal units that are fully free to move and interact, and transmit data wirelessly in real-time or after testing.

References

- Burcharth, H.F., 1985. Fatigue in Breakwater Concrete Armour Units, Proceedings of the 19th International Conference on Coastal Engineering: ICCE '84: Houston, Texas, September 3-7 1984. (pp. 2592-2607). Chapter 174.
- CLI, 2012. Guidelines for Design – Core-Loc™ Design Guide Table, Preliminary Design Guidelines, Concrete Layer Innovations.

- Cornett, A., 1995. A Study of Wave-Inducing Forcing and Damage of Rock Armour on Rubble-Mound Breakwaters, University of British Columbia – Theses and Dissertations, Ph.D. Thesis.
- Cornett, A., Mansard, E., 1994. Wave Stresses on Rubble-Mound Armour, Proceedings of the 24th International Conference on Coastal Engineering, Kobe, Japan.
- Douglas, S., Eden, D., Simpalean, A., Kozlowski, T., Nistor, I., Cornett, A., Anglin, D., Via-Estrem, L., Latham, J.P., Xiang, J., 2019. Conference paper submitted to Coastal Structures 2019, American Society of Civil Engineers Coasts, Oceans, Rivers, Ports Institute.
- Douglas, S., Eden, D., Simpalean, A., Logan, S., Nistor, I., Cornett, A., 2018. Hydrodynamic Analysis of Core-Loc™ Armour Units via Controlled Drop Tests, Proceedings of the 7th International Conference on the Application of Physical Modeling in Coastal and Port Engineering and Science Coastlab18 Conference, Santander, Cantabria, Spain, May 22-26, 2018.
- Hofland, B., Arefin, S., van der Lem, C., van Gent, M., 2018. Smart Rocking Armour Units, Proceedings of the 7th International Conference on the Application of Physical Modeling in Coastal and Port Engineering and Science, CoastLab18 Conference, Santander, Cantabria, Spain, May 22-26, 2018.
- Latham, J.P., Anastasaki, E., Xiang, J., 2013. New Modelling and Analysis Methods for Concrete Armour Units Systems Using FEMDEM, Journal of Coastal Engineering, Vol. 77, Pp. 151- 166.
- Sakakiyama, T., Kajima, R., 1990. Scale Effect of Wave Force on Armor Units. Proceedings of the 22nd International Conference on Coastal Engineering, Volume 22 Chapter 128, 1990, pp. 1716-1729.
- Scott, R.D., Turcke, D.J., Anglin, C.D., Baird, W.F., 1988. Simplified Models for Measuring Armour Unit Forces, Proceedings of the 21st International Conference on Coastal Engineering, June 20-25, 1988, Costa del Sol-Malaga, Spain.
- Van der Meer, J.W., 1988. Stability of Cubes, Tetrapods and Accropode, Proceedings of ICE Breakwaters 1988, Thomas Telford Limited, London, 71-80.
- Van der Meer, J.W., d'Angremond, K., van Nes, C.P., 1994. Stresses in Tetrapod Armour Units Induced by Wave Action, Proceedings of the 24th International Conference on Coastal Engineering, Volume 24 Chapter 123, 1994, pp. 1713-1726.
- Van der Meer, J.W., Heydra G., 1991. Rocking armour units: Number, location and impact velocity. Elsevier Science Publishers B.V. Amsterdam. Coastal Engineering Volume 15, pp. 21-39.